Pergamon

PII: S0191-8141(96)00018-1

Journal of Structural Geology, Vol. 18, No. 7, pp. 925 to 931, 1996

0191-8141/96 $15.00 + 0.00

Rock rheology and sharpness of folds in single layers

LABAO LAN and PETER HUDLESTON

Department of Geology and Geophysics, University of Minnesota, Minneapolis MN 55455, U.S.A.

(*Received* 18 *August* 1995; *accepted in revised form* 26 *February* 1996)

Abstract—Many folds in rocks display angular profiles with sharp hinges and straight limbs. Previous studies by many authors have demonstrated that such fold shapes in *multilayers* result from an intrinsic anisotropy possessed by layered or foliated rocks. Our results of two-dimensional finite-element modeling show that folds with sharp hinges and straight limbs may also develop in *isolated* competent layers under suitable rheological conditions.

Two basic material properties that affect fold shape are non-linearity and anisotropy. Viscous–plastic flow, power-law flow (strain-rate softening), and strain softening are three types of non-linear behavior. All lead to folds with sharp hinges and straight limbs. Anisotropy has a similar influence on fold geometry. Angularity of folds in isolated competent layers increases with increasing non-linearity of the layer or increasing anisotropy of the layer, and a quantitative relationship between fold angularity and degree of non-linearity or anisotropy may be established. Virtually identical angular fold shapes may be produced by either non-linear or anisotropic layer behavior. The strain distribution associated with these shapes is very different, however. For non-linear behavior, strain is focused in the fold hinges and minimal on the limbs, and for anisotropic behavior the reverse is the case, with shear in the limbs being dominant. These differences suggest that it should be possible to distinguish non-linear from anisotropic rheological behavior using layer shape and strain pattern. Copyright © 1996 Elsevier Science Ltd

INTRODUCTION

Fold shape in layered rocks is extremely variable, the shapes of most folds lying somewhere in a wide spectrum from broad rounded hinge zones with short limbs, through sinusoidal forms to angular, narrow-hinge, straight-limbed forms (Hudleston 1973, Ramsay & Huber 1987, pp. 313–314). The aspect of shape we refer to here is the geometric form of individual folded surfaces, as distinct from layer shape which is usually specified in terms of thickness variations of individual layers (Ramsay 1967, pp. 345–351, Hudleston 1973). For specific layer configurations the range in shapes becomes restricted, and it is clear that the layer configuration, and especially layer spacing, has much to do with fold shape (e.g. Biot 1965). As a practical measure of fold sharpness or angularity, we use a sharpness parameter that reflects how curvature is distributed around the fold arc (Hudleston & Lan 1994a, Lan & Hudleston 1995). This parameter, ki, has a value of 1 for a pure chevron fold and 0 for a fold consisting of a circular arc (Hudleston & Lan 1993, 1994a).

We focus in this paper on angular folds, the most striking examples of which are found in multilayers (Fig. 1a). Chevron folds and kink-bands are the two extreme forms of angular fold, and they have been the subject of investigation of many workers, by means of theory (e.g. Biot 1965, Cobbold *et al.* 1971, Johnson & Fletcher 1994), physical experiments (e.g. Cobbold *et al.* 1971, Honea & Johnson 1976, Blay *et al.* 1977) and numerical modeling (e.g. Latham 1985, Ridley & Casey 1989). It is clear from this work that fold angularity is favored by a mechanical anisotropy that results from the alternation of stiff and soft layers in a sequence (e.g. Price & Cosgrove 1990).

In contrast to the angular fold forms found in many multilayers, fold shape in isolated competent layers consists typically of rounded outer arcs and the maintenance of an overall parallel layer geometry (Fig. 1b). This is the case for folding in an isotropic linear viscous or an elastic layer (Ramberg 1964, Hudleston & Lan 1993). However, angular folds may in fact develop in isolated layers under suitable circumstances (Fig. 1c). We summarize in this paper the different ways in which angular folds with sharp hinges and straight limbs can be produced in single layers, and describe how we can distinguish among the factors that cause angularity and thus obtain information on the physical conditions of the rocks at the time of the folding deformation.

WAYS OF DEVELOPING ANGULAR FOLDS IN ISOLATED LAYERS

Plastic yielding

If a stiff layer behaves as a linearly viscous or elastic material with a yield strength, there is the possibility of plastic yield occurring during folding, at the site of greatest stress, which is at the innermost or outermost edges of the layer in the fold hinges. Chapple (1969) demonstrated analytically that this would lead to localization of strain in the hinge and the development of a sharp fold profile for a viscous–plastic material (Fig. 2). The degree of sharpness depends on the fraction of the folding history during which plastic yielding occurs, which in turn depends on the ratio of the yield stress to the applied external load and on the history of application of the load. The fold has a sharper hinge and longer

straight limbs if the ratio of end load to critical load, P/P_c, is large. In the limit it will produce a chevron shape.

Strain-rate softening

A similar effect to plastic yielding occurs for materials with a power-law viscous constitutive relationship. Non-linearity arises naturally from flow involving crystal–plastic deformation. A non-linear flow results in increasingly greater strain rates as bending stresses increase, again in the inner and outer arcs of the folds at the hinges. The higher strain rates lead to larger strains in the hinges and less strains in the limbs, resulting in sharper fold hinges and straighter limbs. For highly non-linear materials, an angular fold profile is formed, as shown clearly using numerical models (Hudleston & Lan 1993, 1994a). The angularity increases systematically as the power-law exponent, n_L, of the stiff layer is increased (Fig. 3, also see Hudleston & Lan 1993, 1994a). We have previously shown (Hudleston & Lan 1993, 1994a) that fold hinge sharpness, for values of $L/h > 10$ and for a wide range of viscosity ratios, is relatively insensitive to viscosity ratio (m), wavelength/thickness (L/h), and fold amplitude. This insensitivity allows linear behavior to be distinguished from non-linear behavior on the basis of fold shape over a wide range of conditions (Hudleston & Lan 1994a). It should be emphasized, however, that the power-law exponent, n_L, also strongly affects the buckling instability and the dominant wavelength of the folds (Fletcher 1974, Smith 1977, Lan & Hudleston 1991).

Strain softening

Neurath & Smith (1982) discussed the effect of strain softening on folding and boudinage. They demonstrated that strain softening is qualitatively and quantitatively similar in effect to strain-rate softening in influencing dominant wavelength selection and fold amplification rates. On the basis of limited numerical modeling we find that increasing the degree of strain softening has an almost identical influence on fold shape as increasing the power-law exponent, n_L, of the stiff layer. This is consistent with the theoretical predictions of Neurath & Smith (1982).

Anisotropy

An alternative way of modifying deformation in the stiff layer and inducing shape changes in folds is by flow anisotropy (Price & Cosgrove 1990). Anisotropic flow might be expected for rocks with a strong shape or crystallographic preferred orientation (Hudleston *et al.* 1996). For such flow, viscosity becomes a tensor quantity. In a coordinate frame parallel to the plane of anisotropy, the viscosity, N, for normal stress is different than that, Q, for shear stress (Cobbold 1976). The degree of anisotropy is given by the ratio $A = N/Q$. We have studied the effect of anisotropy on single-layer folding using a two-dimensional finite element code in incompressible viscous fluids (Hudleston & Lan 1994b). In the models, the plane of anisotropy is kept parallel to the layering as the folds grow.

As might be expected, the numerical results show that increasing the value of A for the stiff layer, or to a lesser extent the matrix, leads to more angular folds with straighter limbs. Figure 4 shows a set of single-layer buckle folds produced in anisotropic linear materials with the same initial configurations and deformation conditions, except for differences in the value of A of the stiff layer and matrix ($A = 1, 20, 50$). Increasing A also increases the buckling instability and, unlike the situation for isotropic flow, the instability does not disappear when $m = 1$ (see Cobbold 1976, Lan & Hudleston unpublished). A more detailed description of the effect of anisotropy on folding and the implications for natural folds will be addressed elsewhere.

Inhomogeneity of layering (effective anisotropy)

A stiff layer may be homogenous and anisotropic, as discussed in the previous section, but it is possible also for an anisotropic 'stiff layer' to be made up of several isotropic sub-layers of different viscosity, that together make the layer effectively anisotropic. Biot (1965 ch. 4) has shown that a multilayer has an effective anisotropy that depends on the viscosities of the layers making up the multilayer, and the proportionate thickness of each layer type in the multilayer. For a multilayer consisting of alternating layers of viscosity μ_1 and μ_2, of fractional thicknesses α_1 and α_2, respectively (Biot 1965, p. 186), $N = \mu_1\alpha_1 + \mu_2\alpha_2$ and $Q = 1/(\alpha_1/\mu_1 + \alpha_2/\mu_2)$. Such a multilayer of finite thickness embedded in a less stiff matrix will behave in a very similar manner to a homogeneous anisotropic stiff layer. Figure 5(b) is a fold in a composite stiff layer made up of five sub-layers whose viscosities alternate between those of the single layer and its matrix that form the fold of Fig. 5(a). The angularity due to the induced anisotropy of the fold in Fig. 5(b) is clear. Thus, it is not necessary for any particular rock type within a stack of layers to be anisotropic for the stack in aggregate to be so.

DISCUSSION

It is apparent from the above that angularity of folds in isolated competent layers can be achieved in a number of different ways. Given natural examples of angular fold shapes, can we distinguish among them? This question is best addressed by comparing folds of nearly identical wavelength/thickness ratio, amplitude, and sharpness produced by the various mechanisms. We show three such folds in Fig. 6, involving three different types of stiff layer behavior in an isotropic, Newtonian matrix. All the folds in this figure developed from the same initial value of initial amplitude (A_o) and initial wavelength/initial

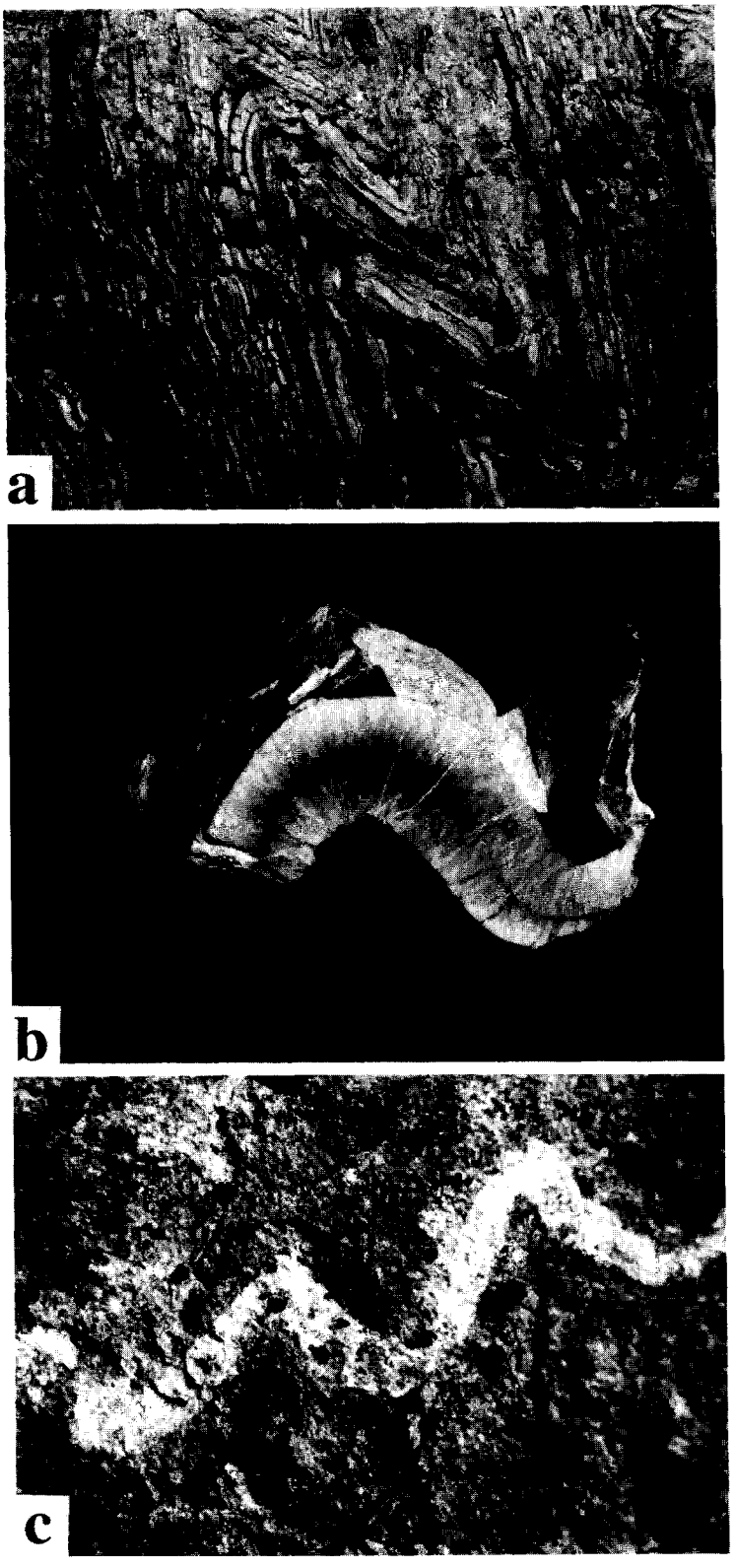

Fig. 1. Natural folds to show variations in shape. (a) 'Angular' folds in a multilayered sequence of siltstones and shales of the McKenzie Formation, Appalachian Valley and Ridge Province, near Pinto, Maryland. (b) 'Rounded' fold in an isolated calcite vein in slates of the Canyon Creek Formation, Rocky Mountains, near Golden, British Columbia. (c) 'Angular' folds in an isolated quartz vein in phyllitic rocks of the Pennine zone, Western Alps, Switzerland.

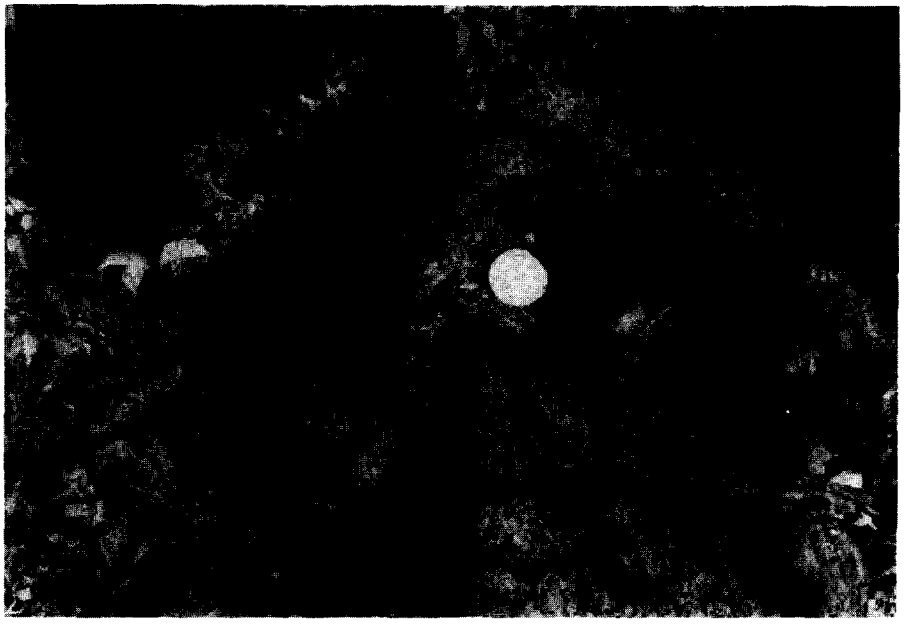

Fig. 7. Outcrop-scale fold in fine sandstone–siltstone layers in shales of the Trimmer's Rock Formation, Pennsylvania, showing fanning of incipient cleavage, especially in the syncline. The average sharpness index, ki, of the four segments of this fold is 0.84. This value is inconsistent with linear rock rheology but consistent with nonlinear or anisotropic rheology. The cleavage pattern is inconsistent with anisotropic rheology of the layer.

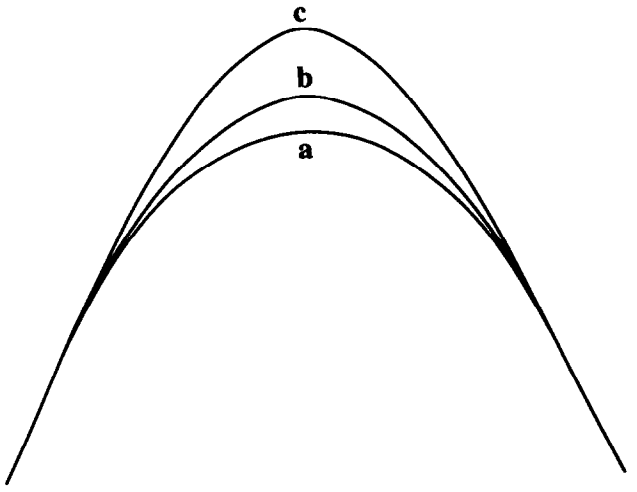

Fig. 2. Three folds, developed analytically in the visco–plastic material, at a limb dip of 60.5° for L/h = 40 and ratio (= 3) of yielding stress to external load. (a) P/P_c = 0.99, (b) P/P_c = 0.999, (c) P/P_c = 0.9999. Here P/P_c is defined the ratio of end load to critical load (after Chapple 1969, fig. 8).

thickness (L_o/h_o). All are relatively straight limbed, and all are significantly different in shape from folds developed in isotropic Newtonian single layers (cf. Fig. 5a). The first example (Fig. 6a) is a single-layer buckle fold with n_L = 10. The second (Fig. 6b) is a fold produced in a homogeneous anisotropic stiff layer, with a ratio of normal viscosity, N, to shear viscosity, Q, of 15. In the third example (Fig. 6c), the folded stiff layer is composite, made up of three stiff layers and two soft layers sandwiched between them, all individual layers being Newtonian isotropic. The soft layers are one-hundredth

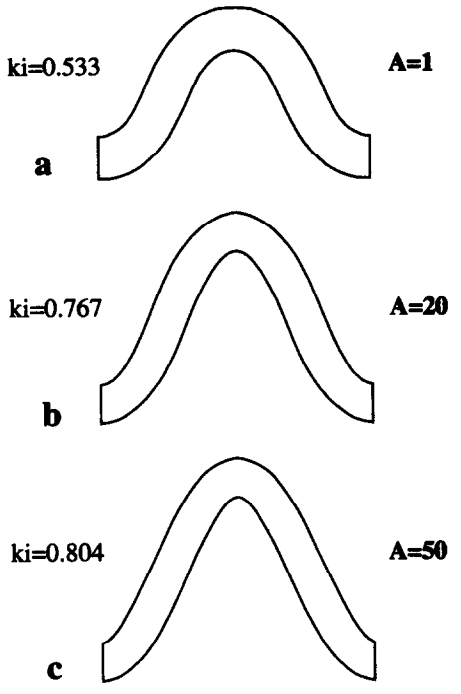

Fig. 4. Angular shape of buckle folds varies with an increasing degree of anisotropy. All started at the same initial configuration (L_o/h_o = 12, A_o = $0.1h_o$), and for the same viscosity ratio (m = 100), and at S = 40%. (a) A = 1, ki = 0.533; (b) A = 20, ki = 0.767; (c) A = 50, ki = 0.804. Again, ki is shown beside each fold. A presents ratios of normal viscosity, N, to shear viscosity, Q, of the layer and matrix.

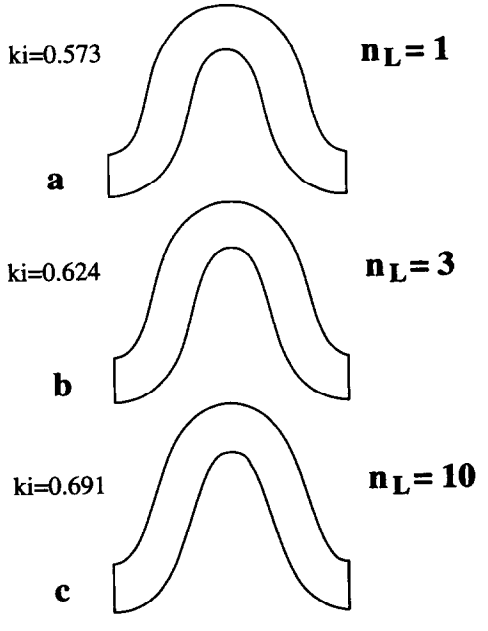

Fig. 3. Fold sharpness, described by ki, increases as the value of the power-law exponent, n_L, of the stiff layer is increased. Three folds developed from identical initial sinusoidal perturbations (L_o/h_o = 12, A_o = $0.1h_o$) and for the same viscosity ratio (m = μ_L/μ_M = 100). All at S = 50% (layer-parallel shortening). (a) n_L = 1, ki = 0.573; (b) n_L = 3, ki = 0.624; (c) n_L = 10, ki = 0.691 (after Hudleston & Lan 1994a, fig. 11).

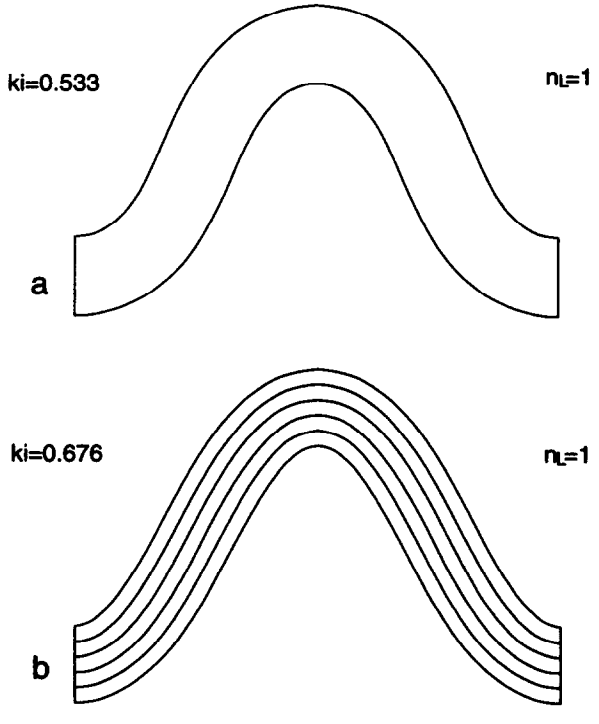

Fig. 5. Fold shapes developed from single-layer (a) and multilayer (b) models for the same initial parameters (wavelength/thickness, L_o/h_o = 12, and amplitude/thickness, A_o/h_o = 0.1) and rheological parameters (n_L = 1 and m = 100). All at S = 40%. The corresponding values of the sharpness index, ki, for individual folds are shown in the figure.

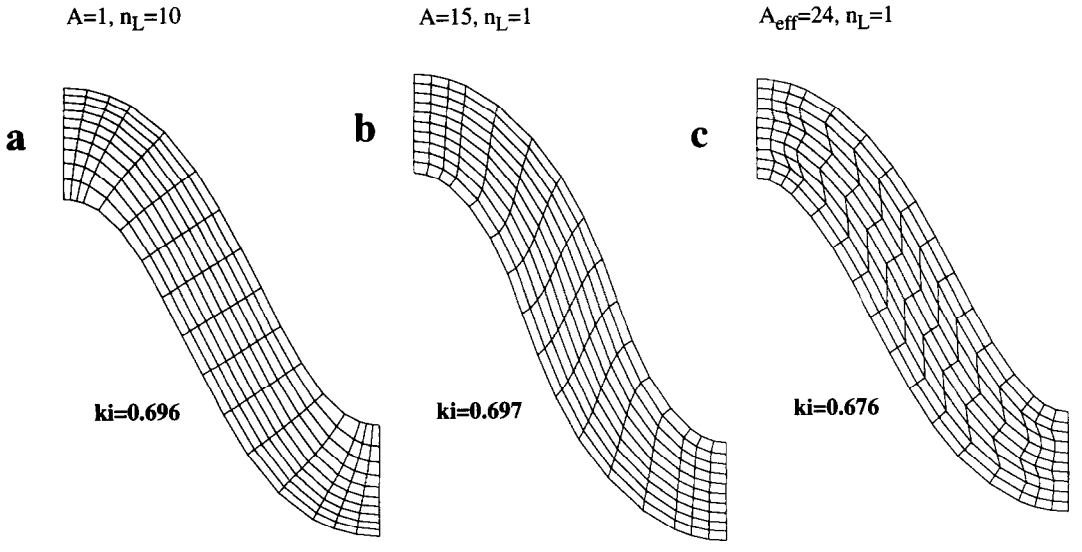

Fig. 6. Buckle folds in isolated stiff layers or packages with sharp hinges and straight limbs produced in three different ways. In all cases L_o/h_o = 12, A_o/h_o = 0.1, m = 100 and S = 40%. The matrix is not shown. (a) Single layer for n_L = 10 (A = 1); (b) Single layer for A = 15 (n_L = 1); (c) Multilayer (3 stiff layers, 2 soft layers with m = 100) for n_L = 1, A_{eff} = 24. The value of sharpness index, ki, is also given beside each fold.

the viscosity of the stiff layers, and the matrix has the same viscosity as the soft layers. The effective ratio of normal viscosity to shear viscosity for the composite layer is about $A_{eff} = (N/Q) = 24$, based on Biot's theory (Biot 1965, pp. 432–433).

The finite element grid lines in our models, originally forming a rectilinear, orthogonal pattern, can be used in Fig. 6 to determine strain (Hudleston & Lan 1994b, Treagus *et al.* 1994). Thus, although the overall fold shapes are similar, the manner in which strain is accommodated in the three folds in Fig. 6 is very different. For non-linear behavior (strain-rate softening), strain is focused in the fold hinges, with significant layer extension in the outer arcs and shortening in the inner arcs; the fold limbs are almost unstained. The mechanism is essentially one of tangential–longitudinal strain (Ramsay & Huber, 1987p. 457–461). For homogenous anisotropic behavior, there is little strain in the hinges, and a large shear strain is developed in the limbs. This is approaching the flexural flow fold mechanism (Ramsay & Huber 1987 p. 445–446, Hudleston *et al.* 1996). For composite anisotropic behavior, the strain alternates between strong layer-parallel shear in the soft sub-layers and tangential–longitudinal strain in the stiff sub-layers. The differences among these folds can thus be established either by direct measurement of strain or by inference of strain from fabric, as for example by the location and orientation of cleavage and small-scale faulting and vein development (see for example Ramsay & Huber 1987, figs. 21.12 and 21.18).

Viscous–plastic behavior, as described by Chapple (1969), and illustrated in Fig. 2, is equivalent to extremely non-linear power-law flow, as $n \rightarrow \infty$ in the flow law. Thus, there is little practical distinction between these. Also, it is in practice probably impossible to distinguish strain-softening from strain-rate softening. Anisotropic behavior, both in homogeneous and inhomogeneous (composite) layers, is however, clearly distinguishable from the other mechanisms of producing angular folds.

We do not have good sets of data on both shape and strain for natural folds that allow full practical demonstration of the points made in this paper. We illustrate a natural fold in Fig. 7, however, for which we can measure shape and make some inference about state of strain, and from this we can make some tentative conclusion about the rheological state of the rock during folding. The fold is in a siltstone in shaly matrix and is viewed parallel to the fold axis. The average value of sharpness index, ki, for the segments of this fold is about 0.84. This high value implies either strongly non-linear rheology or strong anisotropy of the stiff layer. The siltstone has a weak or incipient spaced cleavage that fans around the fold and is strongest in the syncline hinges (Fig. 7). If we make the common assumption that this fabric forms perpendicular to the maximum finite shortening in the rock, that is it forms parallel to the XY plane of the strain ellipsoid, then the strain pattern depicted is one more consistent with tangential longitudinal strain than flexural flow (cf. Fig. 6). We thus conclude that for this fold, non-linear rheology is the likely cause of the relatively angular fold shape.

We have shown here that angular folds in single layers may develop either due to layer non-linearity or due to anisotropy. Fold shape allows us to distinguish linear homogeneous layer behavior from either of these effects, and strain distribution allows us to distinguish non-linear from anisotropic layer behavior. Thus, fold shape and strain distribution provide a tool to determine possible combinations of rheological properties that are able to account for a particular natural fold.

Acknowledgements—We acknowledge support provided by the National Science Foundation (EAR-9017922, EAR-9219702) and the University of Minnesota Supercomputer Institute. We thank Richard Lisle for his comments.

REFERENCES

Biot, M.A. 1965. *Mechanics of Incremental Deformations.* Wiley, New York.

Blay, P., Cosgrove, J.W. & Summers, J.M. 1977. An experimental investigation of the development of structures in multilayers under the influence of gravity. *J. geol. Soc. London* **133**, 329–342.

Chapple, W.M. 1969. Fold shape and rheology: the folding of an isolated viscous–plastic layer. *Tectonophysics* **7**, 97–116.

Cobbold, P.R. 1976. Mechanical effects of anisotropy during large finite deformations.. *Bull. Soc. géol. Fr., 7 Ser.* **18**, 1497–1510.

Cobbold, P.R., Cosgrove, J.W. & Summers, J.M. 1971. Development of internal structures in deformed anisotropic rocks. *Tectonophysics* **12**, 23–53.

Fletcher, R.C. 1974. Wavelength selection in the folding of a single layer with power-law rheology. *Am. J. Sci.* **274**, 1029–1043.

Honea, E. & Johnson, A.M. 1976. A theory of concentric, kink and sinusoidal folding and of monoclinal flexuring of compressible, elastic multilayers. IV. Development of sinusoidal and kink folds in multilayers confined by rigid boundaries. *Tectonophysics* **30**, 197–239.

Hudleston, P.J. 1973. An analysis of single layer folds developed experimentally in viscous media. *Tectonophysics* **16**, 189–214.

Hudleston, P.J. & Lan, L. 1993. Information from fold shapes (in: Special Issue—'Geometry of Naturally Deformed Rocks'). *J. Struct. Geol.* **15**, 253–264.

Hudleston, P.J. & Lan, L. 1994. Rheological controls on the shapes of single-layer folds. *J. Struct. Geol.* **16**, 1007–1021.

Hudleston, P.J. & Lan, L. 1994. The effect of anisotropy on buckle fold development. *Geol. Soc. of Am., Abstracts with Programs* **26**, A315.

Hudleston, P. J., Treagus, S. & Lan, L. (1996). Flexural flow: does it occur in nature? *Geology* **24**, 203–206.

Johnson, A. M. & Fletcher, R. C. 1994. *Folding and Viscous Layers.* Columbia University Press, New York.

Lan, L. & Hudleston, P.J. 1991. Finite element models of buckle folds in non-linear materials. *Tectonophysics* **199**, 1–12.

Lan, L. & Hudleston, P.J. 1995. A method of estimating the stress exponent in the flow law in rocks using fold shape. *Pure Appl. Geophys.* **145**, 620–633.

Latham, J.-P. 1985. A numerical investigation and geological discussion of the relationship between folding, kinking and faulting. *J. Struct. Geol.* **7**, 237–249.

Neurath, C. & Smith, R.B. 1982. The effect of material properties on growth rates of folding and boudinage: experiments with wax models. *J. Struct. Geol.* **4**, 215–229.

Price, N. J. & Cosgrove, J. W. 1990. *Analysis of Geological Structures.* Cambridge University Press, London.

Ramberg, H. 1964. Selective buckling of composite layers with contrasted rheological properties, a theory for simultaneous formation of several orders of folds. *Tectonophysics* **1**, 307–341.

Ramsay, J. G. 1967. *Folding and Fracturing of Rocks.* McGraw-Hill, New York.

Ramsay, J. G. & Huber, M. I. 1987. *The Techniques of Modern Structural Geology*, Vol. 2. *Folds and Fractures.* Academic Press, London.

Ridley, J. & Casey, M. 1989. Numerical modeling of folding in rotational strain histories: strain regimes expected in thrust belts and shear zones. *Geology* **17**, 875–878.

Smith, R.B. 1977. Formation of folds, boudinage, and mullions in non-Newtonian materials. *Bull. geol. Soc. Am.* **88**, 312–320.

Treagus, S., Hudleston, P.J. & Lan, L. 1994. Does flexural flow develop in parallel folds?. *Geol. Soc. Am., Abstracts with Programs* **26**, A316.